

Localization of Multiple Deep Epileptic Sources in a Realistic Head Model via Independent Component Analysis

*David Weinstein†, Leonid Zhukov†,
Geoffrey Potts‡*

*Email: dmw@cs.utah.edu,
zhukov@cs.utah.edu, gpotts@rice.edu*

UUCS-2000-004

†Center for Scientific Computing and Imaging
Department of Computer Science
University of Utah
Salt Lake City, UT 84112 USA

‡Department of Psychology
Rice University
Houston, TX 77005-1892, USA

February 1, 2000

Abstract

Estimating the location and distribution of current sources within the brain from electroencephalographic (EEG) recordings is an ill-posed inverse problem. The ill-posedness of the problem is due to a lack of uniqueness in the solution; that is, different configurations of sources can generate identical external fields. Additionally, the existence of only a finite number of scalp measurements increases the under-determined nature of this problem. Most source localization algorithms attempt to solve the inverse problem by fitting the potentials created on the scalp from multiple dipoles to a single time step of EEG measurements. In this paper we consider a spatio-temporal model and exploit the assumption that the EEG signal is composed of contributions from statistically independent sources. Under this assumption, we can apply the recently derived blind source separation algorithm (BSS), also referred as to Independent Component Analysis (ICA). This algorithm separates multichannel EEG data into temporally independent activation maps due to stationary sources. For our study, we use a 64 channel EEG recording of a multi-focal epileptic event and a realistic geometric model of the cranial volume derived from MRI data. The original ICA algorithm required the number of sources to be equal to the number of recorded channels and becomes unstable otherwise. In this paper, we propose a novel approach for solving this problem through the reduction of the data subspace. Specifically, we discard eigenvectors with small eigenvalues from a PCA analysis of the data prior to ICA decomposition. Our results show that using these proposed subspace reduction methods, multi-focal epileptic data can be successfully decomposed into several independent activation maps. For each activation map we perform a separate source localization procedure, looking only for a single dipole using a multistart downhill simplex method. The localized sources are found to be located and oriented at physiologically appropriate positions within the brain

Introduction

In this paper, we introduce a novel method for localizing epileptogenic sources in patients with multi-focal temporal lobe epilepsy. Localizing multiple deep sources is computationally challenging due to superposition of signal from the active regions and “blurring” of the signal as it projects to the scalp. We address these challenges by incorporating statistical methods to separate the signal into independent activation maps, and by constructing a detailed geometric model of the patient’s head.

The EEG data for our study comes from multi-focal seizure events. As such, it is known in advance that the signal will not be attributable to a single dipole source. Rather, the time series will contain contributions from multiple epileptogenic regions. Each region (representable as a dipole) will have its own independent time course. In order to reduce the noise inherent in the raw data, we perform an eigen-decomposition (PCA) and discard the small components. Having removed the noise, but still faced with a superposition of multiple dipole activations, we perform a blind source separation technique (ICA) in order to separate the sources. The result of this statistical preprocessing of the raw EEG data is a separate activation map for each dipole source. Each activation map is then fed into a source localization algorithm, in order to find the separate epileptic foci.

The source localization algorithm identifies the dipole which, for a particular geometric model, best accounts for the measured EEG signal. Choosing the model requires careful consideration, especially since we know a priori that the sources are likely to be deep relative to the scalp surface. In [Huiskamp, 1997], Huiskamp et al showed that a spherical shell model is not adequate to localize deep temporal lobe sources. Rather, a more realistic patient model was required. Furthermore, because we desire as accurate a source localization as possible, we have chosen to construct a model that incorporates local conductivity anisotropy. Thus, we have opted for a finite element, rather than boundary element model.

Putting the pieces together, we identify multi-focal regions of activation by 1) performing PCA to reduce the data space; 2) utilizing ICA to extract independent activations; 3) constructing a patient-specific finite element model; and 4) localizing each dipole independently with a downhill-simplex search method.

Methods

We begin with the construction of a patient-specific computational model. The realistic head geometry is obtained originally from raw MRI data. This data is then segmented; that is, each tissue material is labeled in the underlying voxels [Wells, 1994]. The segmented head volume can then be tetrahedralized via a mesh generator which preserves the classification when mapping from voxels to elements [Schmidt, 1995]. For each tissue classification, we assign a conductivity tensor from the literature [Foster, 1989]. A cut-through of the classified mesh is shown in Figure 1.

The next step of our method is to preprocess the raw EEG data into independent activation sequences. This processing is done in two stages: PCA and ICA. Once the EEG data has been processed, we will apply a source localization method in order to identify the active region responsible for each activation sequence.

PCA Preprocessing

Let X be a spatio-temporal data matrix, where every row contains voltages at a particular electrode at consecutive time steps and every column contains voltages for all electrodes at some moment in time. We first decompose the initial data into signal and noise subspaces [Mosher, 1992]. This is achieved by finding the eigen-decomposition of the covariance matrix \mathbf{R} , where $\mathbf{R} = \{\mathbf{X}\mathbf{X}^T\}$, and discarding eigenvectors with eigenvalues smaller than some noise threshold. We can estimate an accuracy of such a decomposition by attempting to restore the original signals from this signal subspace; we choose a threshold such that our restoration is at least 98%. Having chosen a subspace, we project the original data onto it: $\mathbf{V}_s = \sqrt{\mathbf{\Lambda}}\mathbf{U}^T\mathbf{X}$, where $\mathbf{\Lambda}$ and \mathbf{U} are the eigenvalues and eigenvectors which form the signal subspace. We now exploit the assumption that the original signals were independent, as it allows us to decompose \mathbf{V}_s into independent components using independent component analysis (ICA) [Bell, 1995].

ICA Decomposition

The ICA algorithm proceeds by finding an unmixing matrix \mathbf{W} , such that rows of the matrix $\mathbf{S} = \mathbf{W}\mathbf{V}_s$ will be independent, i.e. the multivariate probability density function (pdf) of \mathbf{S} is equal to the product of the pdf of each signal in \mathbf{S} . The unmixing $\mathbf{W} = (\mathbf{w}_1, \mathbf{w}_2, \dots, \mathbf{w}_n)$ matrix can be constructed iteratively, for example, by

using a fixed-point algorithm [Hyvarinen, 1997] to compute its columns:

$$\begin{aligned}\mathbf{w}_i(k+1) &= E\{\mathbf{v}(\mathbf{w}_i(k)^T \mathbf{v})^3\} - 3\mathbf{w}_i(k); \\ \mathbf{w}_i(k+1) &= \frac{\mathbf{w}_i(k+1)}{\|\mathbf{w}_i(k+1)\|},\end{aligned}$$

where \mathbf{v} are vectors drawn from the signal subspace \mathbf{V}_s and k is the iteration number. To ensure that at each time we estimate a different independent component, we use a deflation scheme, where we work with the projection onto the subspace orthogonal to already restored components.

Now we can compute independent source signal matrix \mathbf{S} by applying \mathbf{W} to the signal subspace data, $\mathbf{S} = \mathbf{W}\mathbf{V}_s$. To restore the electrode recordings due to just a single source, we zero out all of the rows but one in the signal matrix \mathbf{S} , and compute the back projection:

$$\mathbf{Y}_i = \mathbf{U}\sqrt{\Lambda}\mathbf{W}^{-1}\mathbf{S}_i$$

where the first part of this expression corresponds to back projecting from the signal subspace onto the electrodes. These \mathbf{Y}_i vectors are what we will be trying to reproduce, one at a time, with our simulations.

So, by using signal pre-processing we have effectively reduced the multi-source localization problem to a sequence of single-source localizations. We know the potentials, \mathbf{Y}_i , at the electrodes on the scalp surface and having constructed a geometric finite elements models of the head volume, we now need to find a single dipole which creates that map.

FEM Solution

Mathematically, the problem of computing the electric potentials within the cranial volume due to a set of current sources can be described by Poisson's equation [Plonsey, 1965]:

$$\nabla \cdot (\sigma \nabla \Phi) = \mathbf{J}_s$$

subject to the Neumann boundary conditions:

$$(\sigma \nabla \Phi) \cdot \mathbf{n} = 0$$

everywhere on the scalp except for at the electrodes where the electrostatic potential is known, $\Phi = \phi$; \mathbf{J}_s are the current sources. We can solve this problem using the

finite element method (FEM) to compute a solution within the entire volume domain [Jin, 1993]. Using FEM we obtain the system of equations:

$$\mathbf{A}_{ij}\phi_j = \mathbf{b}_i,$$

where \mathbf{A} is a stiffness matrix, \mathbf{b} is a source vector and ϕ is a vector of unknown potentials at every node. The \mathbf{A} matrix is sparse (for our simulation, it contained approximately 2,000,000 non-zeroes entries), symmetric and positive definite. We solve the above system using LU-decomposition, or, since the matrix \mathbf{A} is symmetric positive definite, Cholesky factorization. This allows us to use multiple right hand sides for the same stiffness matrix without re-factorizing it, thus minimizing our computational overhead.

Source Localization

To compute the solution of the described inverse problem, we find the set of dipoles which generate the “best fit” (minimal error) of computed electrode potentials to measured electrode potentials. We use correlation coefficient CC , as our error metric.

$$CC = \frac{\sum_i |\mathbf{Y}_i - \phi_i|}{\|\mathbf{Y}\| \cdot \|\phi\|},$$

where ϕ_i is the result of the forward model computation (as described in the subsection above) for a particular dipole source. A value of $CC = 1$ indicates that the simulated and recovered values at that time instant are identical up to a scaling factor.

Previously, finding this minimum requires solving the forward problem for every possible configuration of a large number of dipoles. However, because of our statistical preprocessing, we only have to find one dipole for each activation map. Each dipole in the model has 6 parameters: 3 location coordinates (x, y, z) , 2 degrees of orientation (θ, ϕ) , and the dipole strength, P . We will use first 5 as the parameters for the source localization process. We do not need to optimize for the dipole strength, since strength will not effect our error metric. Rather, P can be recovered as a post-process, after the optimal dipole position and orientation have been determined. We use the downhill simplex method [Nedler, 1993] to find the minimum of the multidimensional cost function.

Discussion

This study has proposed a novel method for source localization of multiple independent, stationary sources. We have applied this method to the localization of dipolar epileptic foci and have successfully recovered independent sources for each focus, as shown in Figure 2. The positions of the foci correspond to the temporal lobes, preliminarily indicating the qualitative accuracy of our method. This demonstrates the importance of using a realistic head model with anisotropic conductivities. As a future study, we will compare the results of our method with results generated from BEM models and FEM models without anisotropy.

References

- [Huiskamp, 1997] Huiskamp, G.G.M. and Maintz, J.B.A. and Wieneke, G.H. and Viergever, M.A. and van Huffelen, A.C. The influence of the use of realistic head geometry in the dipole localization of interictal spike activity in MTLE patients, *NFSI 97*, 84-87, 1997.
- [Wells, 1994] Wells, W.M. and Grimson, W.E.L. and Kikinis, R. and Jolesz, F.A. Statistical intensity correction and segmentation of MRI data, *Visualization in Biomedical Computing*, 13-24, 1994.
- [Schmidt, 1995] Schmidt, J.A. and Johnson, C.R. and Eason, J.C. and MacLeod, R.S. Applications of automatic mesh generation and adaptive methods in computational medicine, *Modeling, Mesh Generation, and Adaptive Methods for Partial Differential Equations* Babuska, I. et al. editors, Springer-Verlag, 367-390, 1995.
- [Foster, 1989] Foster, K.R. and Schwan, H.P. Dielectric properties of tissues and biological materials: A critical review, *Critical Reviews in Biomed. Eng.* 17, 25-104, 1989.
- [Mosher, 1992] Mosher, J.C. Lewis P.S. and Leahy R.M. Multiple dipole modeling and localization from spatio-temporal MEG data, *IEEE Trans. Biomed. Eng.* 39, 541-57, 1992.
- [Bell, 1995] Bell, A. and Sejnowski, T. An information-maximization approach to blind separation and blind deconvolution. *Neural Computation*, 7:1129-1159, 1995.
- [Hyvarinen, 1997] Hyvarinen, A. and Oja, E. A fast fixed-point algorithm for Independent Component Analysis *Neural Comp.* 9,1483-1492, 1997.

[Plonsey, 1965] Plonsey, R. Volume Conductor Theory, *The Biomedical Engineering Handbook* J.D. Bronzino, editor, 119-125, CRC Press, Boca Raton, 1995.

[Jin, 1993] Jin, J, *The Finite Element Method in Electromagnetics* John Wiley and Sons, 1993.

[Nedler, 1993] Nedler, J.A. and Mead, R. A simplex method for function minimization, *Compt. J* 7, 308-313, 1965.

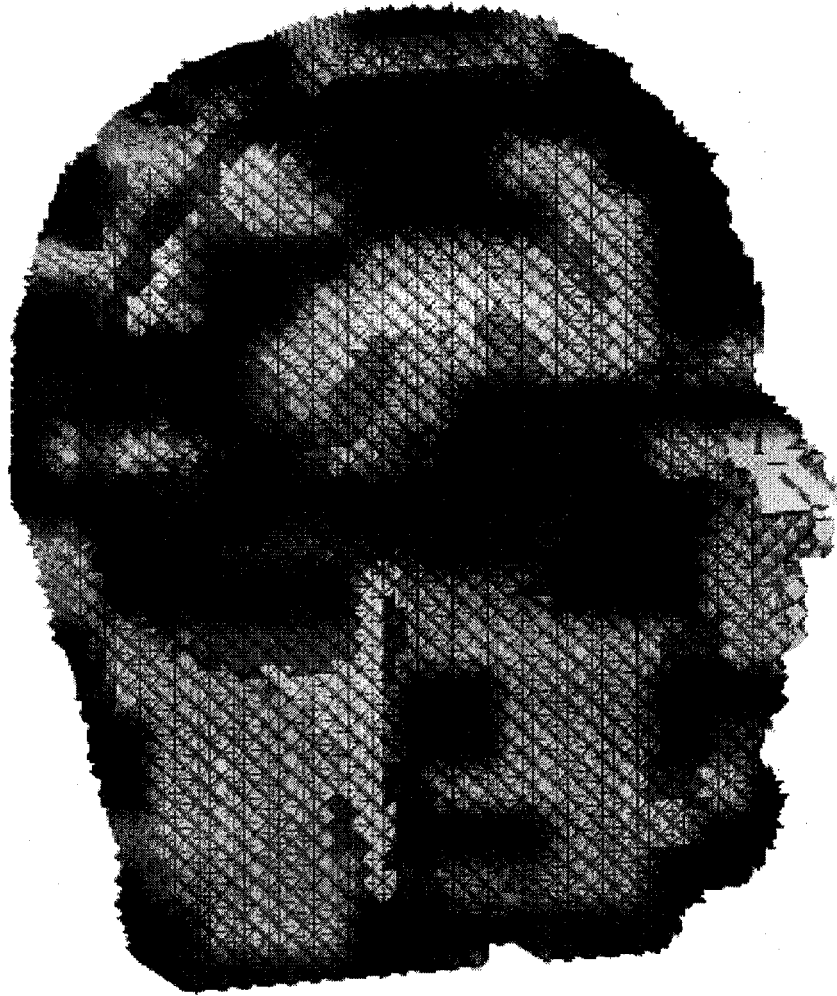


Figure 1: Cut-through of the finite element. The full model contains approximately 164,000 nodes and 768,000 elements. As indicated by gray-scale coding, each element is assigned a conductivity tensor according to its underlying anatomic tissue.

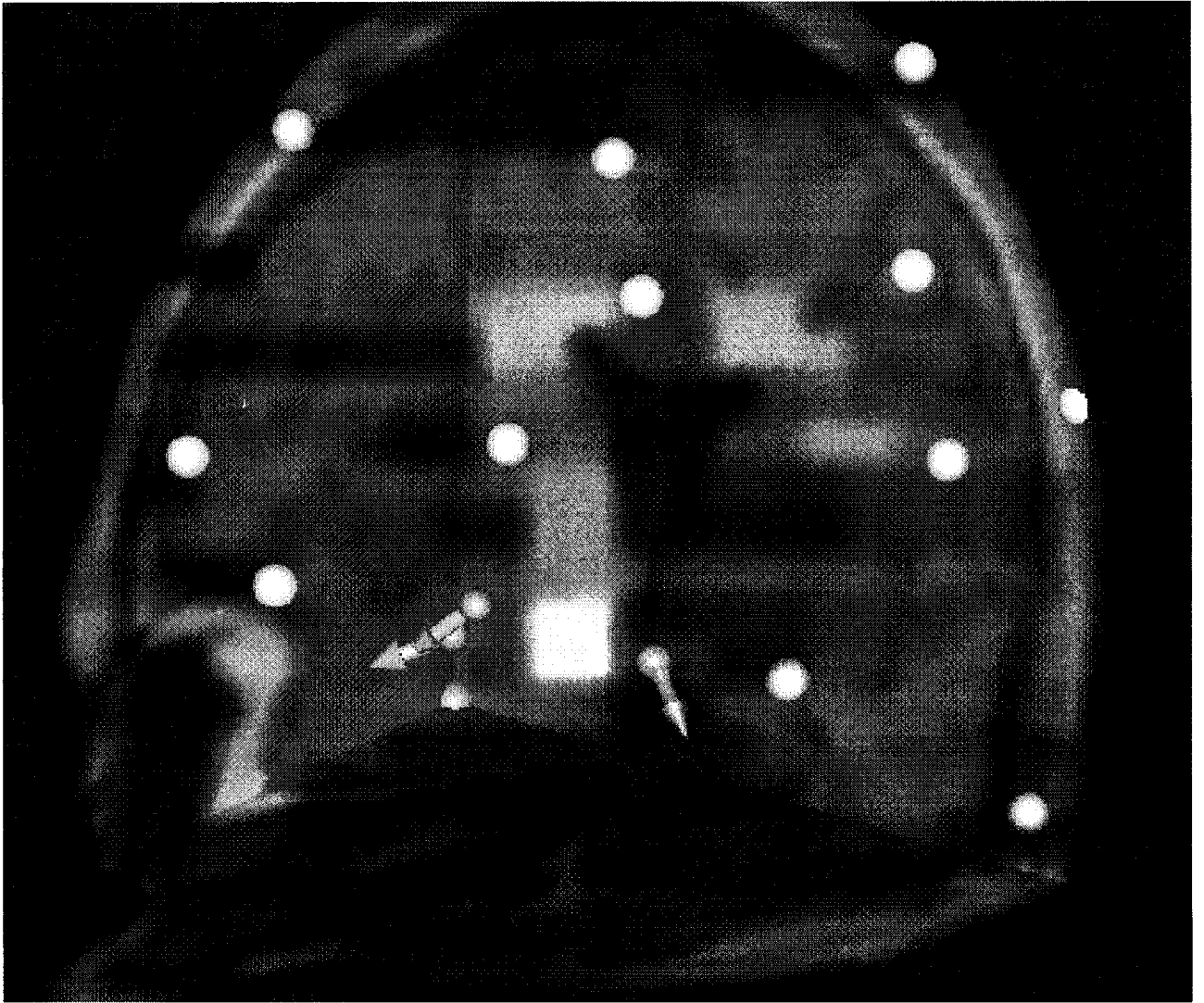


Figure 2: Three dipole sources (arrows) localized within the temporal lobes. Orthogonal MRI slices(background) and electrode positions (spheres) are shown for reference.